Available online at www.sciencedirect.com
SCIENCE DIRECT
Earth and Planetary Science Letters 237 (2005) 710–728
EPSL
www.elsevier.com/locate/epsl

The memory of volcanic waters: Shallow magma degassing revealed by halogen monitoring in thermal springs of La Soufrière volcano (Guadeloupe, Lesser Antilles)

Benoît Villemant [a,b,c,*], Gilbert Hammouya [b], Agnès Michel [a], Michel P. Semet [a,b], Jean-Christophe Komorowski [a,b], Georges Boudon [a,b], Jean-Louis Cheminée [b,1]

[a] *Institut de Physique du Globe de Paris, CNRS, Equipe de Volcanologie, 4 pl. Jussieu, 75005 Paris, France*
[b] *Observatoires Volcanologiques et Sismologiques, IPGP, France*
[c] *Université P. & M. Curie, Paris, France*

Received 7 September 2004; received in revised form 7 April 2005; accepted 9 May 2005
Available online 18 July 2005
Editor: V. Courtillot

Abstract

The halogen contents of thermal waters collected since 1979 at La Soufrière volcano (Guadeloupe, Lesser Antilles) are interpreted as a retarded record of magma degassing pulses dispersed into the hydrothermal system. The further the spring is located from the source, the larger the time delay and the older the event recorded in water chemistry. Using advection–dispersion transport models in porous media, we reconstruct the time-series of degassing pulses for the period 1971–1992 and show that it correlates with the seismic records. The 1975–1977 sismo-volcanic crisis at La Soufrière is thereby interpreted as the result of a magma intrusion at shallow depth (~3 km) which likely began in approximately 1973 and degassed in a pulsatory regime during ~15 yr. The recent recrudescence of fumarolic and seismic activity could represent the initial stage of new magma injection. Measurement of halogen contents in hydrothermal waters collected around active volcanoes may provide a powerful tool for detection of the initial stages of magma intrusions.

Keywords: volcanic activity; hydrothermal systems; halogens; volcano monitoring

The difficult and controversial management of the 1975–1977 sismo-volcanic crisis at La Soufrière volcano in Guadeloupe is still very present in the mind of the volcanologists community. It was essentially due to the poor knowledge at the time of the behaviour of such volcanic systems. However, the origin of this crisis has never been unambiguously identified [1,2]. Since this period, a large number of other volcanic crises have been more successfully managed. But the problem of prediction remains an

* Corresponding author.
E-mail address: villemant@ipgp.jussieu.fr (B. Villemant).
[1] Deceased.

0012-821X/$ - see front matter © 2005 Elsevier B.V. All rights reserved.
doi:10.1016/j.epsl.2005.05.013

extraordinarily difficult task especially for the seldom erupting explosive andesitic volcanoes. It is well examplified by the on-going crisis at the nearby Soufriere Hills volcano in Montserrat [3] where eruptive scenarios for lava dome forming eruptions must be regularly revisited because unexpected new phases of activity occur since 1996. Despite the large spectrum of monitoring techniques, the interpretation of geophysical and geochemical information to forecast volcanic activity remains a complex task. For instance, at La Soufrière, seismic signals, considered as the best indicators of impending volcanic activity, did not provide unequivocal information even a short time before the volcanic crisis [1,2]. At Soufriere Hills, seismic activity could not be interpreted to forecast the first lava dome extrusion [3]. Similarly, ground deformation signals did not provide clear indications of shallow magma emplacement or movement during most part of the on-going volcanic activity [4]. Furthermore, no interpretable precursory signals in the physical and chemical characteristics of thermal springs were recorded before the onset of magmatic activity [5,6]. Some other recent examples (Mt. Pinatubo crisis, Unzen crisis etc.) show that research of precursors to volcanic eruption is a very active domain in volcanology of obvious general interest with societal consequences. For example, recent studies [7] suggest that some observations of tephra before the Mt. St. Helens eruption in May 1980 could have been considered as indications of a magmatic eruption in a near future. The major problem remains the correct interpretation of the monitored signals in terms of deep volcanic processes such as new magma injections, pure hydrothermal activity or any intermediate situation. In this paper we show that systematic and high resolution geochemical monitoring of spring waters around active volcanoes is of major interest for understanding the mechanisms involved during volcanic crises and may provide predictive information.

Along with seismology and geodesy, gas studies play an important role in volcano monitoring especially for detecting degassing of shallow magma intrusion. CO_2 and SO_2 are generally considered as the best indicators [8] because they are of pure magmatic origin contrary to H_2O. However, thermochemical modelling shows that decompression, cooling, oxidation processes, interactions with wall-rocks or hydrothermal systems, and mixing with air, lead to large variations in the concentration and speciation of most volatile components in plumes [9]. The initial gas composition is generally strongly modified at the sampling points, unless direct sampling of erupting magmas may be performed. Magma degassing may also be recorded in hydrothermal systems because water efficiently scavenges volcanic volatiles [10,11]. But here again, the high reactivity of most volatile species, especially SO_2 and CO_2, with thermal waters and solids of the percolation medium renders the recognition of initial gas composition particularly difficult (e.g. see [8,12,13]). Such surveys also generally represent technical challenges due to sampling conditions and analytical difficulties.

The halogens are of particular interest in studies of H_2O-rich magma degassing because they display relatively simple behaviours:

- halogens are mainly extracted from magmatic melts during H_2O degassing as halogen acids,
- H_2O vapour–melt partition coefficients of halogens (except F) are much greater than 1 ($d^{F}_{v-m} \ll 1 \ll d^{Cl}_{v-m} < d^{Br}_{v-m} \ll d^{I}_{v-m}$ [14,15]),
- halogen acids are relatively stable species in H_2O-rich volcanic gases and their abundance are not strongly affected by cooling, decompression, gas–air mixing or solid–gas interactions [9],
- because of their very high solubility in water, halogen acids are completely scrubbed from volcanic gases by interaction with hydrothermal systems in which halogen ions are conservatively transported [11].

From these properties, one may expect that halogen contents and especially their abundance ratios are only slightly modified from their initial values in relatively high temperature gases (say >200 °C) and almost completely preserved in hydrothermal systems which have interacted with volcanic gases at high temperature. In addition, there is a large spectrum of analytical techniques for measuring halogen contents in hydrothermal waters (e.g. see [16]) or in volcanic plumes (e.g. see [17,18]). The survey of halogen contents in thermal springs may thus provide a simple and efficient tool to follow shallow magma degassing activity, especially when it is only represented by low temperature fumaroles. This is particularly valuable

for andesitic volcanoes situated in tropical zones, as in the Lesser Antilles Arc, where volcanic edifices are abundantly drained by meteoric waters and develop a prominent hydrothermal system.

Here we show that monitoring of Cl contents of thermal springs of La Soufrière in Guadeloupe, performed since 1979, allows to trace the evolution in time and space of magma degassing at shallow depth. The transfer of halogens from the magma to the superficial phreatic systems is modelled by an advection–dispersion process. The degassing pulses are correlated with the shallow depth seismic activity. The reconstructed pulsatory regime is interpreted in terms of crystallization induced degassing of a magma intrusion. We conclude that the evolution of halogen concentrations in thermal waters over periods of months to years may be used as indicators of subsurface magmatic activity and trace the evolution of new magma intrusions.

1. The recent volcanic activity at La Soufrière of Guadeloupe

All of the Holocene activity of La Soufrière took place inside La Grande Découverte caldera which formed approximately 50 kyr ago [19,20]. The last magmatic activity took place around 1440 AD inside a horseshoe-shaped depression (Amic crater) inherited from a 3100 yr B.P. flank collapse. The historic activity, recorded since 1635, consists in several phreatic eruptions. The most violent of them occurred in 1797–1798 and 1975–1977. A permanent and well-developed hydrothermal system is evidenced by numerous thermal springs and an intermittently active fumarolic field (Fig. 1). During the 1975–1977 crisis, the summit and flank fumarolic activity was sustained during all the explosive phreatic phase (July 1976–April 1977 [1]). The summit fumaroles vanished in May 1977 and the peripheral fumarolic activity progressively concentrated in the SE sector were it remained residual since 1983. The summit fumaroles were progressively reactivated in 1992, with a persistent high flux of HCl-rich H_2O vapour since late 1997 [20,21].

The distribution of thermal springs around the lava dome is controlled by the basement of the volcanic structures (caldera and flank collapse craters) and the large development of argillic hydrothermal alteration (Fig. 1). Three surveyed springs are located at high altitudes (1170–950 m) within the Amic crater at a maximum distance of 1.2 km from the summit lava dome: Carbet Echelle (CE), Bains Jaunes (BJ), Galion (GA). One spring, close to the second Carbet water fall (CC), is located at a much lower altitude (~590 m) at a distance of around 2.5 km east of the summit. The Bains Chauds du Matouba (BCM) spring is located outside the Amic crater but still within the Grande Découverte caldera, and the Habitation Revel (HR) spring lies outside this caldera. All these springs have relatively high and constant flow rates ranging from ~0.1 l/s for CE to 2.5 l/s for GA–BJ. The main geochemical characteristics of thermal springs and fumarolic fields indicate that all these fluids are mixtures between meteoric and magmatic components [22–24]. The present day summit fumaroles are H_2O-rich vapours (93–99%) containing CO_2, HCl and H_2S. The presence of a minor sea water component and the origin of HCl are still debated [24,25]. However, HCl-rich gases characterise magma degassing at high temperature in some island arc volcanoes as Augustine, Alaska [26], and Soufriere Hills, Montserrat [17,27].

Three main types of thermal waters are defined on the basis of major element compositions [10,22,24]: $Ca–SO_4$ waters (BJ, CE, GA, BCM) close to La Soufrière lava dome, interpreted as mixtures between meteoric water and oxidized H_2S bearing fluids; a $Ca–Na–HCO_3$ water (HR) corresponding to shallow regional groundwaters heated through volcanic heat transfer; a Ca–Na–Cl water (CC), interpreted as a mixture between $Ca–SO_4$ waters and Na–Cl waters

Fig. 1. (a) Sketch map of La Grande Découverte-La Soufrière volcano and location of hot springs around La Soufrière lava dome. Springs labels as in the text. The circles correspond to the projection on the horizontal plane of distances between the unknown fissural feeding conduit and hot springs. They are calculated from the transport model assuming straight and subhorizontal paths (except for CC spring where a source depth of ~3 km is assumed) and a same mean transport rate (see Table 2). (b) Schematic E–W cross-section showing the possible course of fluids in the deep and superficial hydrothermal system and the strong compartimentation of the circulation zones in the edifice.

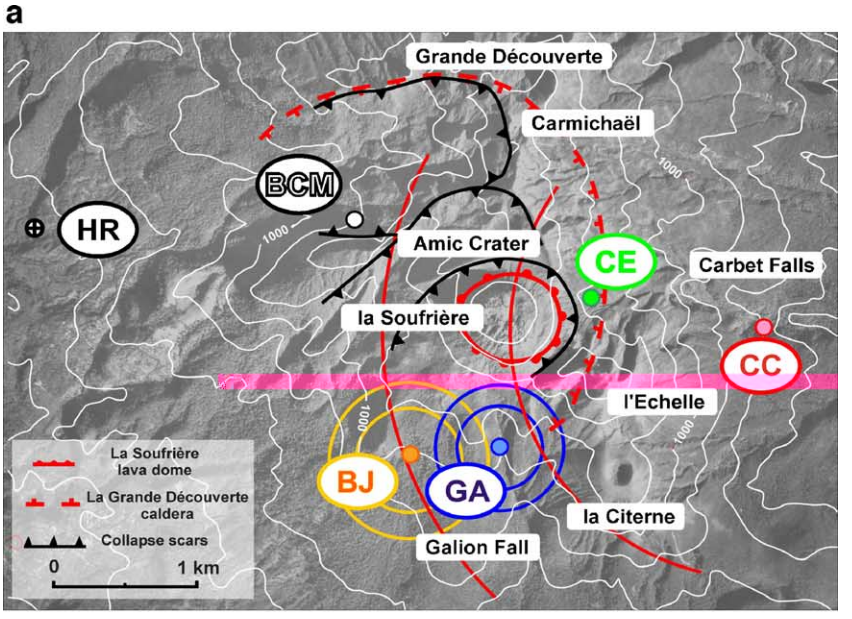
a
Grande Découverte
Carmichaël
BCM
HR
Amic Crater
CE
Carbet Falls
la Soufrière
CC
l'Echelle
BJ
GA
la Citerne
Galion Fall
1000
La Soufrière lava dome
La Grande Découverte caldera
Collapse scars
0
1 km

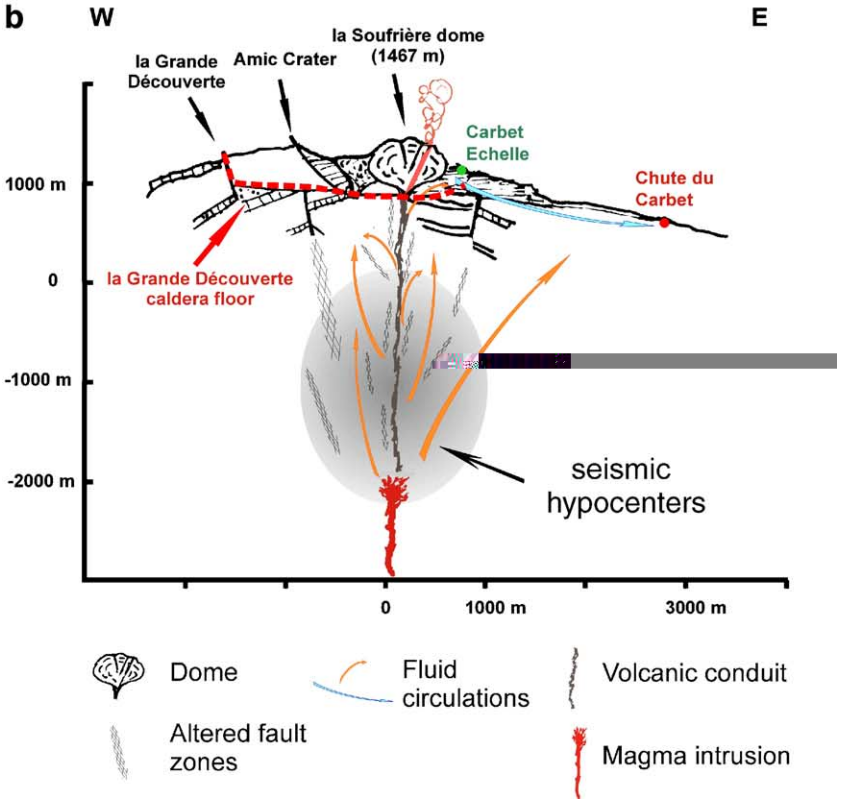
b
W
E
la Soufrière dome (1467 m)
la Grande Découverte
Amic Crater
Carbet Echelle
Chute du Carbet
1000 m
0
-1000 m
-2000 m
la Grande Découverte caldera floor
seismic hypocenters
0
1000 m
3000 m
Dome
Fluid circulations
Volcanic conduit
Altered fault zones
Magma intrusion

the deep geothermal system of

onitoring of thermal springs

among the best surveyed volcano in
n array of surveillance methods
the 1975–1977 volcanic crisis by
Volcanologique de La Soufrière de

Guadeloupe” (G-IPGP) [1,20,21,25]. Permanent networks mo seismicity and ground deformations. Therma ings and fumaroles are sampled and analysed forthnightly base since 1979 providing a conti s data record over ~25 yr. These analyses have complemented by new Br measurements in ve samples (see Annex 1). Data ranges and m values are reported in Table 1.

Large Cl a variations are present in proximal thermal spring t are insignificant for springs loca-

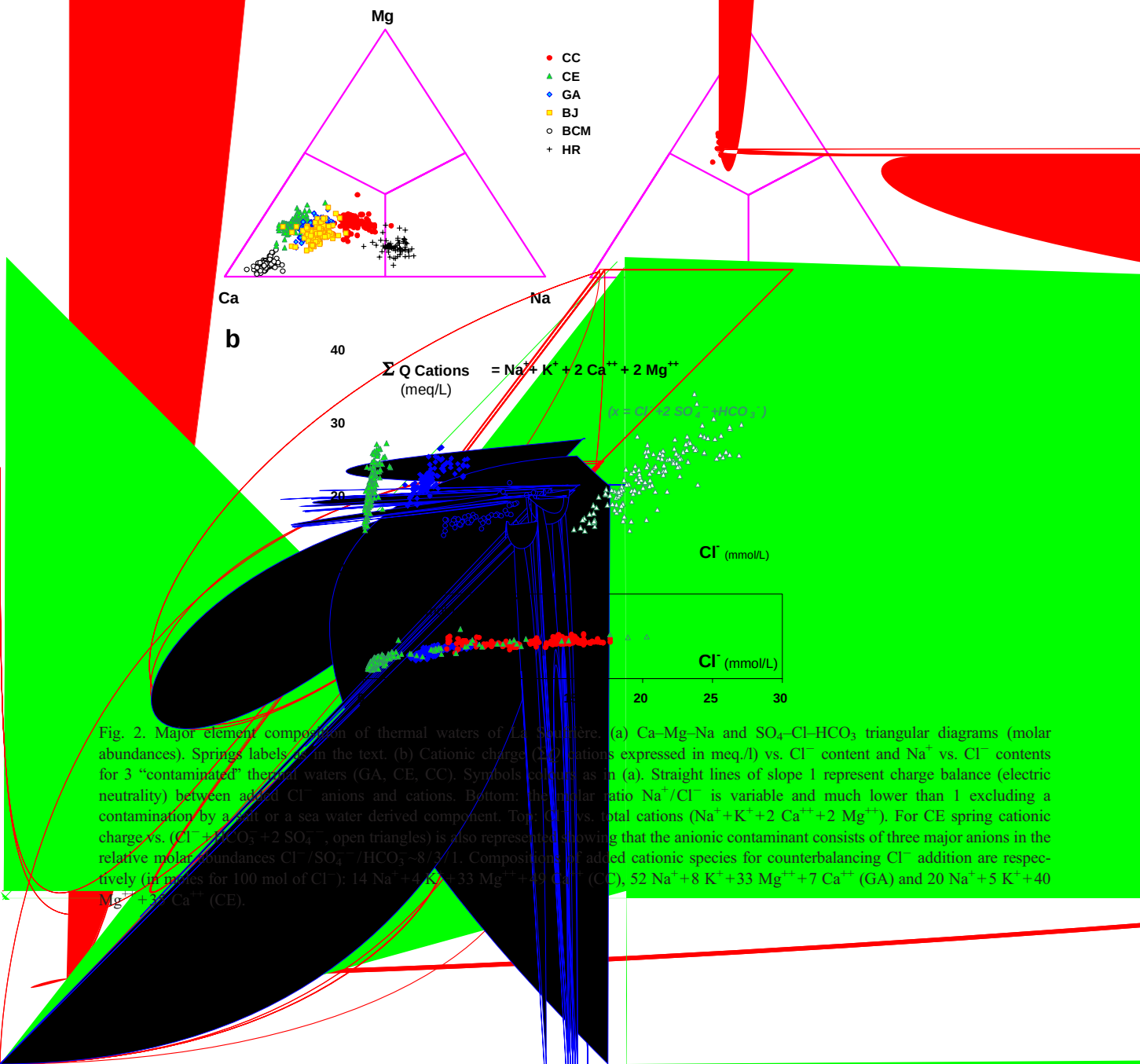

Fig. 2. Major element composition of thermal waters of La Soufrière. (a) Ca–Mg–Na and SO_4–Cl–HCO_3 triangular diagrams (molar abundances). Springs labels as in the text. (b) Cationic charge (2Q cations expressed in meq./l) vs. Cl^- content and Na^+ vs. Cl^- contents for 3 “contaminated” thermal waters (GA, CE, CC). Symbols colours as in (a). Straight lines of slope 1 represent charge balance (electric neutrality) between added Cl^- anions and cations. Bottom: the molar ratio Na^+/Cl^- is variable and much lower than 1 excluding a contamination by a salt or a sea water derived component. Top: Cl^- vs. total cations (Na^++K^++2 Ca^{++}+2 Mg^{++}). For CE spring cationic charge vs. (Cl^-+2 SO_4^{--}+HCO_3^-, open triangles) is also represented showing that the anionic contaminant consists of three major anions in the relative molar abundances $Cl^-/SO_4^{--}/HCO_3^-$~8/3/1. Compositions of added cationic species for counterbalancing Cl^- addition are respectively (in moles for 100 mol of Cl^-): 14 Na^++4 K^++33 Mg^{++}+49 Ca^{++} (CC), 52 Na^++8 K^++33 Mg^{++}+7 Ca^{++} (GA) and 20 Na^++5 K^++40 Mg^{++}+35 Ca^{++} (CE).

Table 1
Mean values and ranges of temperature, pH, major elements and halogens contents of thermal waters of La Soufrière (samples collected between 1979 and 2000)

	T (°C)	pH	Na (mmol/l)	K (mmol/l)	Mg (mmol/l)	Ca (mmol/l)	Cl (mmol/l)	HCO3 (mmol/l)	SO4 (mmol/l)	F (ppm)	Cl (ppm)	Br (ppm)
CC												
Mean	45.4	6.59	4.32	0.64	3.11	4.26	9.66	2.23	2.52	~0.16	341	0.90
Sigma (%)	2	2	8	16	18	19	43	10	15		43	30
Min.	39.5	6.2	3.0	0.3	1.8	2.5	4.1	1.8	1.7	0.15	145	0.40
Max.	46.9	7.3	5.3	0.9	4.9	6.9	17.7	2.8	4.2	0.22	628	1.58
CE												
Mean	36.4	5.70	2.31	0.24	3.27	6.19	3.79	2.57	10.54	~0.03	134	0.23
Sigma (%)	40	3	41	27	19	14	107	34	18		108	159
Min.	21.2	5.3	1.0	0.0	1.4	4.5	0.3	0.3	6.5	0.02	9	0.18
Max.	69.0	6.5	5.9	0.5	5.8	8.3	20.3	4.7	15.9	0.03	720	1.62
GA												
Mean	42.7	4.78	3.26	0.51	3.27	5.99	8.82	0.35	7.93	0.5	312	0.44
Sigma (%)	2	4	15	19	14	7	50	49	16	15	50	70
Min.	39.0	4.3	2.1	0.1	1.8	4.4	2.5	0.0	4.1	0.4	87	0.19
Max.	45.2	5.8	4.4	0.9	5.1	7.2	16.8	0.9	10.0	0.6	596	1.08
BJ												
Mean	26.7	5.07	1.68	0.16	1.39	2.99	2.82	0.24	3.99	0.32	99	0.16
Sigma (%)	5	3	11	31	25	23	45	25	12	19	45	37
Min.	24.0	4.5	1.1	0.1	0.7	2.1	1.0	0.1	2.6	0.18	35	0.09
Max.	31.0	5.7	2.5	0.5	4.0	8.6	5.5	0.7	5.8	0.51	195	0.39
BCM												
Mean	57.5	5.90	1.48	0.19	0.60	6.63	0.59	0.31	7.16	1.83	21	
Sigma (%)	4	3	18	23	24	5	7	25	9	9	8	
Min.	51.8	5.5	1.1	0.1	0.3	6.0	0.5	0.03	5.4	1.08	17	
Max.	59.5	6.5	2.2	0.3	0.9	7.1	0.7	0.7	8.3	2.07	26	
HR												
Mean	32.6	6.68	1.02	0.09	0.26	0.51	0.30	1.84	0.16	~0.05	10	
Sigma (%)	3	3	11	81	37	14	8	10	29		10	
Min.	30.3	6.2	0.7	0.02	0.09	0.40	0.24	1.27	0.07	0.04	6	
Max.	35.5	7.2	1.3	0.57	0.84	0.68	0.36	2.36	0.29	0.05	13	

Sigma values are in %; large sigma values indicate large composition variations with time (see Figs. 2 and 3).

ted outside Amic Crater (Fig. 3a). Concentration maxima are reached at times increasing with the distance to the summit dome. The temporal spread of the maxima also increases with distance. The principal Cl anomalies consist in a series of pulses which are well individualized in the most proximal spring (CE) but fade out in more distal springs (e.g. CC). Over the whole sampling period, F contents and Cl/Br ratios remain constant in all springs (Fig. 3b). The other major anionic species, HCO_3^- and SO_4^{2-}, do not display such anomalies, except in CE where they are correlated to the halogens. The halogen behaviour suggests an origin from the same contaminating source which is likely a juvenile volcanic gas from several lines of evidence: (i) the absence of F enrichments is consistent with the F-depletion of volcanic gases relative to melts [28]; (ii) the Cl–Br and Cl–F correlations exclude contamination by sea water but are consistent with mixing between meteoric water and an 'andesitic fluid' which composition is estimated from degassing models [15,28] (Fig. 3d); (iii) the absence of F and Na enrichments excludes the input

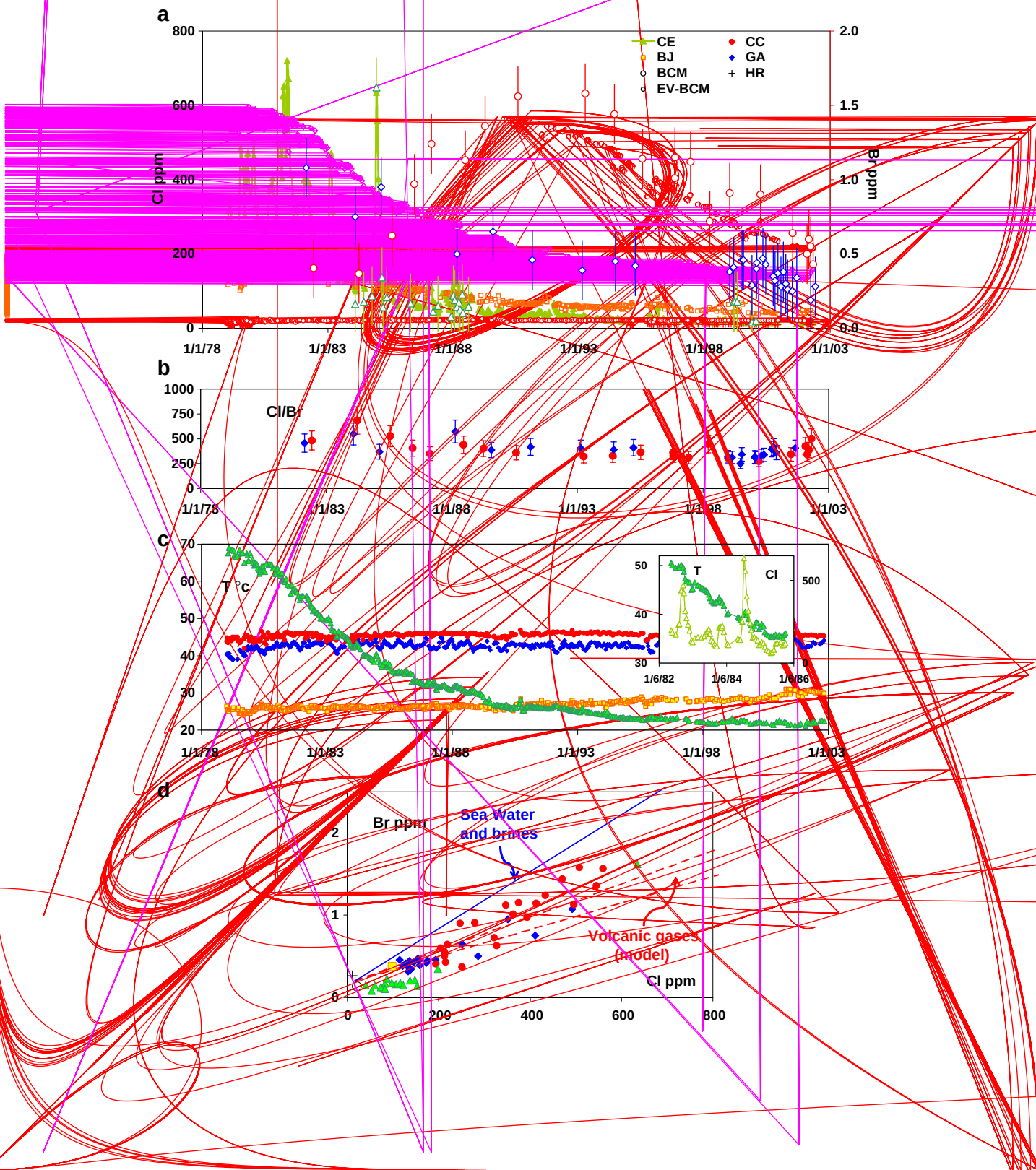
a
CE
CC
BJ
GA
BCM
HR
EV-BCM
Cl ppm
Br ppm
800
600
400
200
0
2.0
1.5
1.0
0.5
0.0
1/1/78
1/1/83
1/1/88
1/1/93
1/1/98
1/1/03
b
Cl/Br
1000
750
500
250
0
c
T °C
70
60
50
40
30
20
T
Cl
1/6/82
1/6/84
1/6/86
d
Br ppm
Sea Water
and brines
Volcanic gases
(model)
Cl ppm
2
1
0
200
400
600
800

of sea water or brines derived from sea water (Fig. 2b); (iv) more generally, the absence of systematic correlations between halogen excesses and contents in a specific cation, indicates that the contaminant cannot be a salt. The cationic species which counterbalance the Cl^- excesses differ from one spring to the other (Fig. 2b) suggesting that a unique HCl-rich fluid contaminant has reacted (by H^+/cations exchanges) with materials of varying compositions depending on the course of the fluid through the volcanic edifice. The long-term storage of such HCl-rich fluids before transportation would have produced a 'contaminant' of homogeneous cationic composition which is not the case.

It is assumed that the different Cl and Br anomalies observed in hot springs result from the emission of a series of fluid pulses by a common magmatic source at depth. These fluids are transported to the surface through fractures and by convecting pore waters, where they mix with superficial groundwaters. During the process, Cl^- and Br^- ions are conservatively transported from the deep gas source to the surface. On the contrary, the S-bearing volatile species and CO_2 rapidly react with thermal waters and solids: they are only present in significant amounts (as HCO_3^- and SO_4^{2-}) in the most proximal spring (CE). CE also displays a large temperature excursion (T_{max}~70 °C for a present day temperature ~23 °C, Fig. 3c) directly correlated with the main Cl anomaly, contrary to other springs (variations of 2–3 °C for temperatures ranging between 25 and 45 °C). It indicates that, contrary to other springs, magmatic fluids are rapidly transferred to CE feeding aquifer.

3. Halogens transport in the volcanic edifice

The transport of conservative ions as halogens by water flow in a porous medium may be described, as a first approximation, by a two-dimensional advection–dispersion model (see Annex 2). [Cl] follows a characteristic anomaly whose maximum, time spread and time delay mainly depend on distance between spring and Cl-injection point (Fig. 4a). Fig. 4b presents the evolution of two major Cl pulses transported at different distances (~75 and ~2000 m) at a flow rate $U/\omega R = 10^{-5}$ ms^{-1}, which fit the signals observed in both CE and CC springs. The Cl pulses are fitted on CE spring record, by adjusting their injection times at $x=0$ and their relative mass fractions (Q). Then they are propagated to distances 25 times longer, approximating CC spring-dome distance. Absolute amounts of Cl transported in distal springs are much lower than for proximal springs and dispersions are much larger (compare Figs. 2 and 4b). On this basis, a direct model has been developed which fits the concentration variations of four springs (CC, CE, GA, BJ, Fig. 4c, Table 2) with the following assumptions:

- Cl evolution in all springs are due to a common series of instantaneous degassing pulses,
- the mass of Cl in each pulse is variable, but, from this common source, the relative mass fraction injected in each spring is constant over the whole time-series,
- the flow parameters ($U/\omega R$) are constant and identical for all springs,
- transport conditions between the injection point and the different springs only differ by the time delay (or path length which is equivalent because of the constant $U/\omega R$) and α values varying in a narrow range (20 m for the most proximal spring, CE and 30 m for other springs),
- as indicated by annual flow rates variations, the variations of surficial groundwater reservoirs volumes are of second order relative to Cl contents variations and thus neglected.

The CE spring is used for fitting a first time-series (1979–1992) of degassing pulses and their relative

Fig. 3. Variations of halogen contents and temperature of spring waters with sampling date. Symbols as in Fig. 2a. (a) Cl (solid symbols) and Br (open symbols); for Cl error bars are within the symbol size. (b) Cl/Br mass ratio in CC and GA spring waters. (c) Temperature (°C). Thermal anomalies are of low amplitude except for the CE spring of which proximal position to the 1976 eruption vents explains the large thermal conductive anomaly not directly related to pulse gas injections. Inset: examples of correlation between large Cl and small T anomalies in CE spring. (d) Br vs. Cl contents of La Soufrière spring waters. Comparison with mixing trends of typical "uncontaminated" groundwaters (BCM and HR) with sea water and brines (solid line) or with volcanic gases (dashed lines); compositions of volcanic gases are calculated from degassing model of andesitic magmas [15,28].

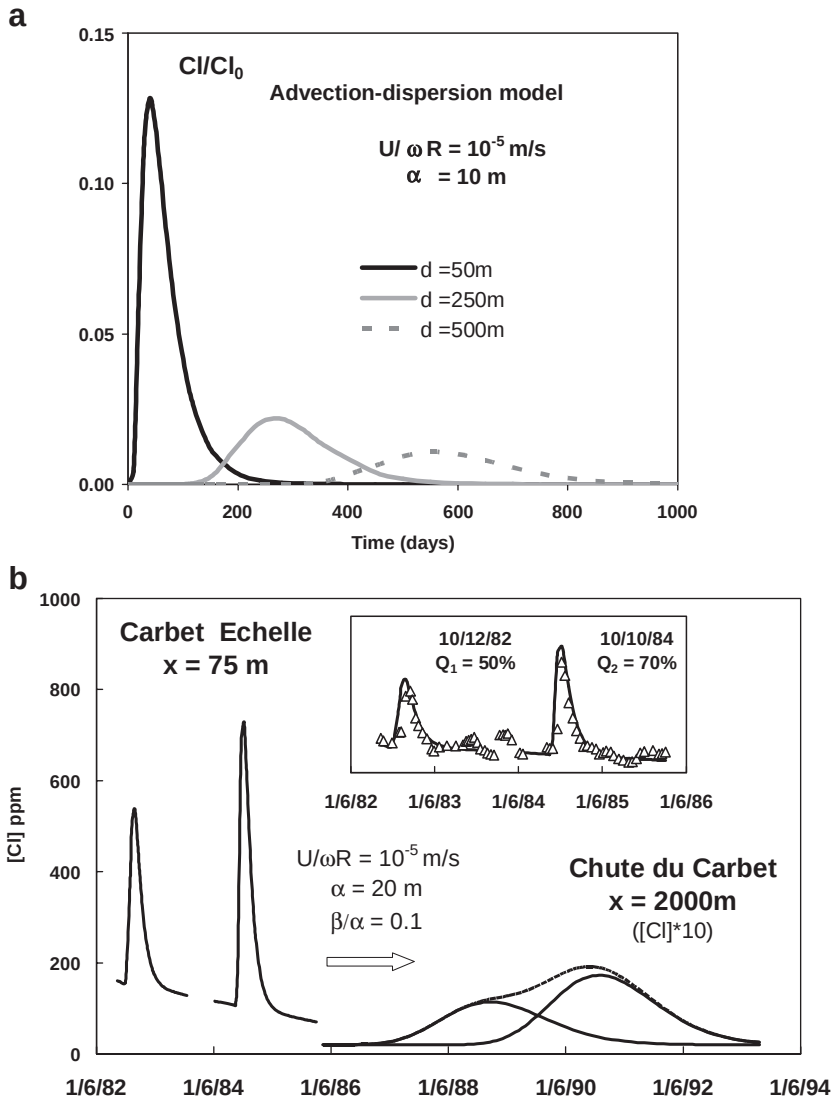

Fig. 4. Advection–dispersion model. (a) Characteristic evolution of a shape of a Cl anomaly generated by a gas pulse injection (at $t=0$) in a water flow with time/distance from the source. Cl contents are calculated relative to the total amount of Cl transported in the direction x. (b) Transport modeling of two major Cl anomalies in CE and CC springs. Cl pulses are fitted on CE spring record (peaks on the left side and Inset) and propagated (arrow) to distances approximating CC spring-dome distance (peaks on the right; absolute Cl contents multiplied by 10; dashed line: peak sum). (c) Fit of advection–dispersion models for CE, GA, BJ and CC springs from the same initial pulse injection times series (see Table 2 for parameters definitions). Top: data and fitting curves; thin lines represent Cl concentrations calculated from individual pulses; they are plotted without the background. Their summation and the addition of a constant background generate the black solid line (best fit). Grey dotted lines: summation of pulse time-series for the 1978–1992 period (CE spring fit) and 1973–1977 period (CC spring fit; see text and Table 2 for explanations). Dotted black line: ideal model assuming identical relative intensities in all thermal springs (bold values in Table 2); the best fit model (black lines) has been obtained by slightly modifying some of the reference intensities (italic values in Table 2). These slight discrepancies indicate local second order variations of volcanic edifice permeabilities inducing slight variations in injected HCl mass fractions. Bottom: fitting residues R=(measured value-best fit value); mean square reduced residuals: MSRR=$\Sigma(R^2/2\sigma^2)$.

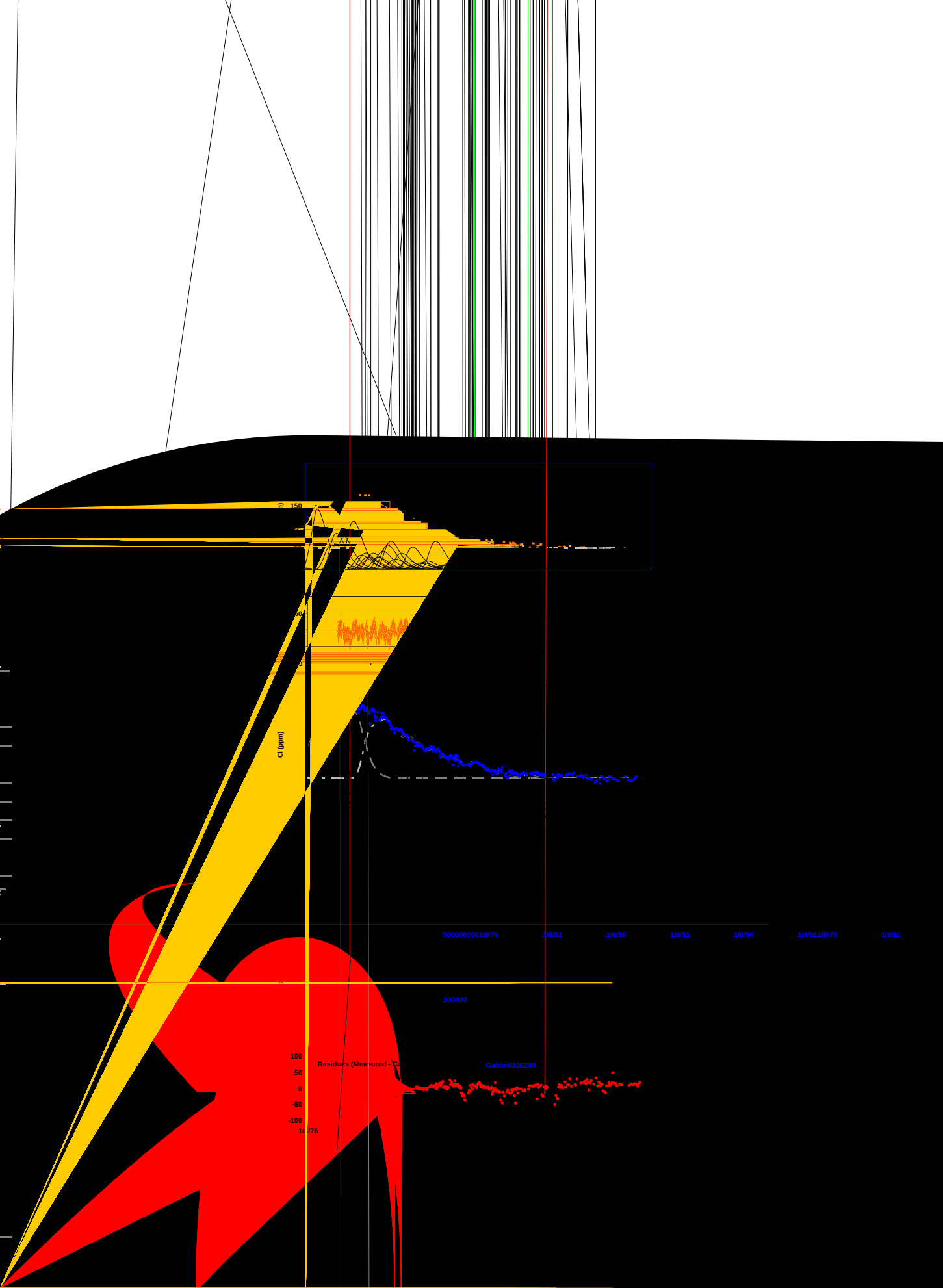
150
Cl (ppm)
5006007001/8/76
1/8/81
1/8/86
1/8/91
1/8/96
1/8/011/8/76
1/8/81
300400
100
50
0
-50
-100
Residues (Measured -
Galion0100200

Table 2
Advection dispersion model (flow parameters and Cl input time series used for fit)

a. Flow parameters used for the different springs

Spring	CE	CC	BJ	GA	Total
Flow (l/s)	0.2	0.01	2.5	1.5	
Time delay (months)	3	148	27	25	
Path length (m)	75	3900	700	650	
α	20	30	30	30	
X_{Cl}	0.4%	1%	32%	66%	100%
M_{Cl} (10^3 kg)	1	2	93	190	286

b: Time series of gas pulse injections and their relative intensities

1) Fit using CE spring

	15/4/79	15/6/79	1/9/79	16/11/79	15/4/80	15/8/80	1/1/81	1/4/81	15/8/81	1/2/82	15/8/82	15/12/82	16/6/83	2/10/83	1/2/84
CE	**40**	30	**30**	40	**30**	**45**	60	70	25	40	20	55	15	16	20
CC				30	20	40	50	60							
BJ	50			60			40	50							
GA	50						50	30	30						

	1/10/84	10/4/85	1/11/85	1/4/86	15/11/86	15/6/87	15/11/87	1/8/88	1/10/89	1/6/90	2/4/91	15/11/91
CE	70	8	15	10	15	10	25	10	5	2	5	6
GA	50			25								

2) Fit using BJ spring

	1/7/75	1/8/76	1/1/77	1/8/77	1/5/78	15/12/78
CE		60	90	80	120	35
CC		40	80	80	110	35
BJ	**150**	**100**	**20**	**40**	**180**	**20**
GA		60	90	80	120	35

3) Fit using an arbitrary time series of 2 injections/year

	1/12/70	1/7/71	1/12/71	1/7/72	1/12/72	1/7/73	1/12/73	1/8/74	1/10/74
CC	**10**	**20**	**10**	20	**20**	**30**	30	20	20

a: Spring flow rates are mean values (data from [21]). Time delay refers to the difference between the time of a gas pulse injection at depth and the time of its appearance as a Cl anomaly in the spring water composition. Indicative path lengths are calculated from these delays using $U/\omega R = 10^{-5}$ ms^{-1}. M_{Cl} represent the mass fractions of Cl injected in each source and X_{Cl} the relative mass fractions; they are calculated for each spring using the Cl anomalies fit and the mean flow rate. No direct information exists on the fraction they represent relative to the total amount of Cl injected in the volcanic edifice (see also Annex 2).
b: Relative intensities (arbitrary units) are indicated for the reference spring (bold numbers). Other springs intensities are quoted only if they differ from the reference value (see text for explanations).

intensities (Table 2). Relative pulse dates are determined from Cl anomaly maxima observed on CE spring record (Fig. 4b). The time delay (~90 d) is determined in order to fit the shape of the main isolated Cl anomalies (Eq. 1, Annex 2). The series consists in ~30 events between December 1978 and August 1988. The second series (1975–1978) is similarly fitted from BJ and GA springs records. Larger time delays of 2 and 2.25 yr respectively are requested to fit the larger dispersion. To fit the complete record of these two springs, the series must be completed by 5 new injections between July 1975 and May 1978. Fitting the Cl record in CC spring requires a time delay of ~12 yr and the addition of a 3rd series of Cl injections dating back to 1970. Due to signal degradation with distance and reduction of the time resolution, these additional pulses are approximated by a series biennal injections. The use of a slightly higher α value for fitting remote springs (BJ, GA and CC, Table 2) is consistent with the usual observation of an increase of α values with transport distances in porous media.

The model indicates that variations of Cl contents in spring waters of La Soufrière are related to a

magma degassing in a pulsatory regime (>45 pulses) lasting ~15 yr (Fig. 5a). This time period encompasses the 1975–1977 sismo-volcanic crisis during which the mass of Cl injected in the phreatic system is maximum (~35% of the total amount). An apparent relative minimum in Cl injections occurs during the culmination of the crisis (July–August 1976) which was characterised by continuous gas venting and phreatic explosions: in that period feeding fissures were largely opened allowing direct degassing to the atmosphere thereby significantly reducing the amounts of fluid injected in the edifice interior. The geometry of the injection zone may be estimated by computed time delay and corresponding source–spring paths lengths (Table 2, Fig. 1) which suggest a 'fissural' feeding source straight below the lava dome, passing between GA and BJ springs and close to CE spring (Fig. 1).

4. Comparison with the seismic record

The time-series of Cl injections given by transport modelling is compared to the seismic record in Fig. 5a. Most of these earthquakes have magnitudes lower than 2 and their hypocenters are restricted in a narrow region under La Soufrière lava dome at ~3 km depth. Only some of the major earthquakes in July and August 1976 had hypocenters that migrated from greater depth (~6 km) to 2 km [29]. Deep hypocenters may have also been recorded at the onset of the 1975–1977 eruption sequence that began by a seismic swarm in July 1975 or perhaps even earlier. There is a close correlation between seismic data and the time-series of Cl injections during the 1970–1992 period. In contrast, a different pattern of activity has been observed recently from 1992 to the present characterized by an increase in seismicity and summit fumarolic degassing strongly enriched in HCl which is not associated to any significant chemical anomalies in proximal springs [29]. These results allow a reappraisal of the models previously proposed for explaining the 1975–1977 crisis which is related either to a new magma injection or a particular stage in the evolution of a deep magma [1], or to the cyclic heating and pressurisation of the hydrothermal system due to heat supply from depth [2].

5. Magmatic- versus hydrothermal-origin of Cl anomalies

The recent studies of Phlegrean Fields activity [30] provide a good reference for the behaviour of a large hydrothermal system controlled by the injection of deep hot fluids which induce thermal and geochemical anomalies registered in surficial systems (diffuse degassing, temperature gradient, deformation etc.). This system is characterized by large and long period anomalies in chemistry (typically ~5 yr), heat flow and local deformations. In addition, modelling indicates that in such systems thermal anomalies should survive long after deep thermal feeding has ceased. These characteristics are not observed in La Soufrière for the 1979–1992 record period. In particular the thermal anomalies (Fig. 3c), except for CE spring, are very low (<5 °C) and have much shorter characteristic durations (6 yr at maximum) than those of the bulk chemical and seismological perturbations (~15 yr). They are not correlated to seismic or chemical signals. In CE spring (Fig. 3c, inset) only short-period temperature anomalies are correlated to the largest Cl anomalies which indicates the rapid and direct input of hot and Cl-rich pulses in its aquifer. Thus we consider that the almost pure chemical anomalies observed at La Soufriere hot springs are better interpreted if a series of separated gas pulses of magmatic origin and carrying a low thermal energy but large volatile contents (CO_2, SO_2, halogens) are directly injected in the volcanic edifice. Most of their travel path to surface likely occurs through fissures associated with very high ascent rates. Thus magmatic fluids are transported through a porous but highly compartimented medium to the surficial phreatic systems. The chemical heterogeneity of the transport medium explains the large variations in the inherited compositions in nonconservative ions (cations balancing acid gases input). Consistently, the thermal anomalies are only preserved for the most proximal spring (CE) corresponding to the lowest transport duration or shortest path.

Melts involved in the recent magmatic activity at La Soufrière in 1440 AD are H_2O- and SiO_2-rich and saturated with water at pressures corresponding to depths ~6–7 km [20]. The extraction of halogens from these melts is controlled by H_2O degassing [28]. Thus, the pulsatory regime of Cl injections during the 1970–1992 period may directly reflect

the step degassing of such a magma intruded at shallow depth. During each degassing step, fluid pressure will increase to generate new fractures or reopen existing fissures. This will allow rapid transfer of fluids and decompression. The overpressure-driven fracturing and the injection of high pressure fluids in the volcanic edifice may be the main source for the observed seismic activity, thus suggesting that a small magma body was stored just beneath the seismogenic zone, at a depth of ~3 km below the summit of the lava dome (Fig. 1b). As demonstrated by the on-going eruption at Soufrière Hills, which is similar to the last magmatic event at La Soufrière of Guadeloupe [20], such small volume magma bodies involved in these eruptions cannot be easily detected by geophysical methods other than seismology (such as deformation and gravimetry) even when magma reaches shallow depths [3,4].

A model with two different degassing regimes is proposed: (i) a decompression induced degassing regime due to magma ascent and (ii) a long-term step degassing regime controlled by magma cooling and crystallization.

6. Decompression induced degassing

The emplacement of a batch or successive batches of magma at shallow depth (~3 km) from a magma chamber at ~6–7 km depth where it is H_2O saturated, induces gas exsolution and overpressures. The exsolved amounts of gas are simply a function of the mass of magma and the H_2O saturation values at initial and final depths (Table 3). An open system degassing process is assumed. All gas fractions generated during this step are continuously extracted through fissured surrounding and ascend almost isothermally at a rate controlled by the permeabilities of the magma and the surrounding rocks and by the overpressure [31]. The characteristic time of fluid escape is lower than 1 d for realistic conditions (see Annex 3). It is also controlled by the diffusion rate of volatiles in the melt and by the degassing-induced melt crystallization [32–34] which have slightly longer time constants (within some days). Both mechanisms of fluid transfer through the magma body and through open fractures in the volcanic edifice are very rapid and similar in duration.

7. Degassing–crystallization model

This second regime corresponds to the long-term step degassing of the static magma body stored at shallow depth. It is induced by heat loss and melt crystallization in a closed system which leads to a fluid overpressure until surrounding rocks fracture and gas escapes. The subsequent closure of the fractures initiates a new pressurisation cycle. This regime is controlled by the magmatic fluid overpressure, the tensile strength of the host-rock and the melt crystallization rate [35,36]. Different theoretical models [35–38] describe the gas production as the result of crystallization, the accommodation of gas exsolution by gas compression in the bubbles, elastic deformation of liquid, crystals and surrounding rocks, and possibly magma contraction accompanying crystallization. The last two processes are negligible for H_2O-rich rhyolitic melts [36]. For simplification, it is assumed that crystallization only occurs in response to heat loss but degassing-

Fig. 5. Comparison of Cl pulses time-series with the seismic records and crystallisation–degassing model. (a) Open triangles: Cl injections time-series deduced from transport modelling (arbitrary scale). Grey bars: number of seisms per month (log scale). For the period of interest (1970–2000) a standardised seismic data set has been built from the different available data sources [21], excluding data with a mean energy per seism corresponding to magnitudes <1. Solid line: exsolved gas mass fractions calculated from the degassing model. The model assumes two degassing regimes (Table 3): (i) magma intrusion at shallow depth between 1973 and 1976 with instantaneous degassing (dashed line) and (ii) a long-lived (1976 to 1992) crystallisation–degassing process (dotted line). Inset: reconstructed time-series of Cl injections (relative masses, arbitrary units) in the different aquifers, taking into account for the different spring flow rates (Table 2). (b) Comparison of data measured from the reconstructed Cl injection time-series (solid circles) with data calculated from the crystallisation–degassing model (open circles). Top: time delays (in days) between two successive gas injections; black dots: pure crystallization–degassing regime; grey circles: period of superimposed magma injections and crystallization–degassing regime; these pre-1979 data are only indicative since the injection time-series is poorly constrained (see Fig. 3 and text). Bottom: comparison of extracted volatile (Cl or H_2O) mass fractions (arbitrary units); the model assumes constant [H_2O] and [Cl] in the residual melts. (c) Evolution of overpressure, temperature, viscosity, and crystal contents in the magma intrusion during the crystallization–degassing regime.

induced crystallization should also be taken into account in more realistic models [32]. The assumed model described in Annex 4, is calculated numerically from a simplified formulation of Tait's model [36] and the evolution of overpressure with time is compared to a given fracture criterion. The main factors controlling the time delay between two fracturation events are: (i) the kinematic viscosity which

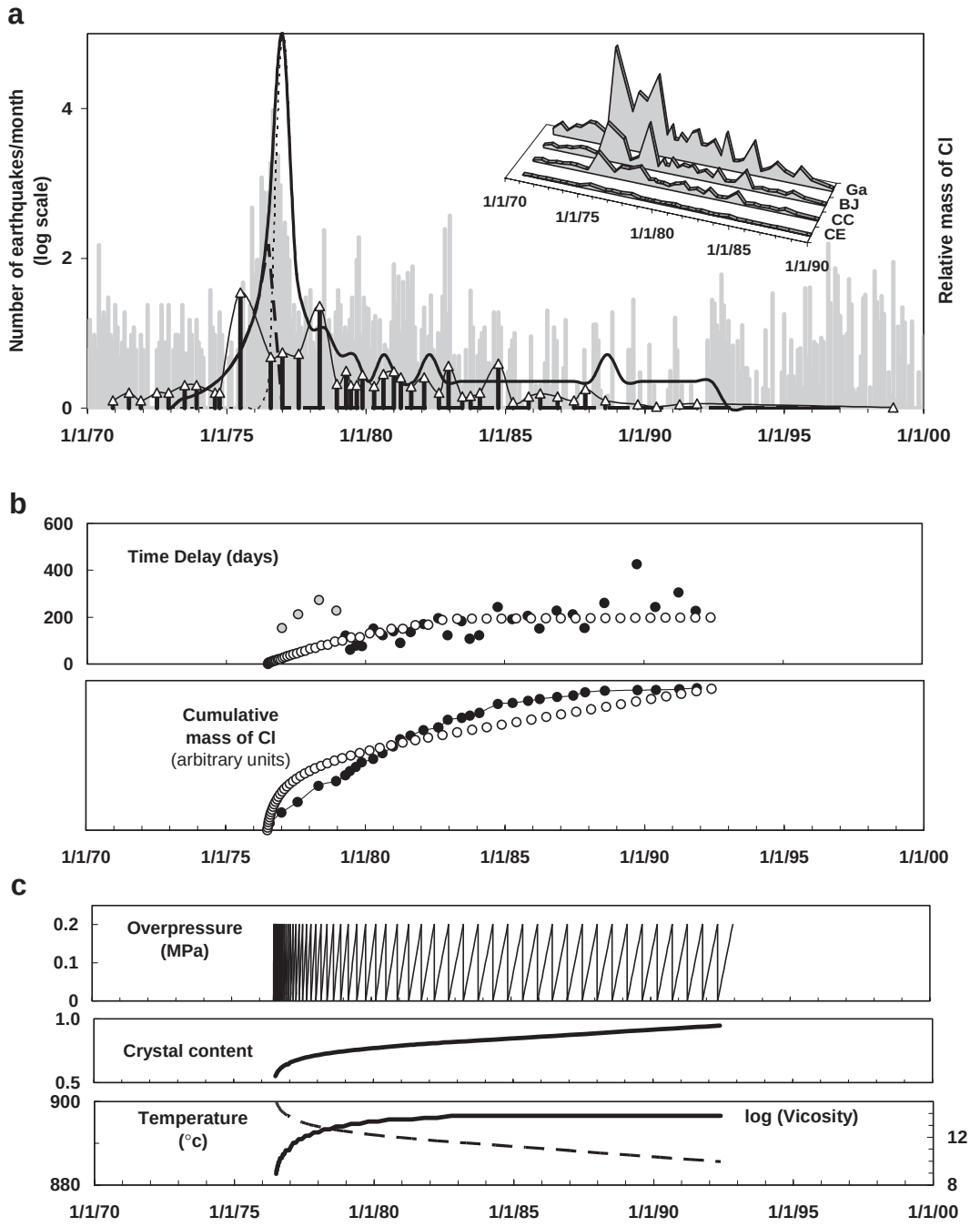

Table 3
Parameters of the degassing models

First and last magma input (rate: **4 intrusions/year**)	01/01/1973	01/07/1976
1) Magma intrusion — 1st degassing regime		
Relative mass fractions	**(1.5%)**	**(30%)**
P_0 and depth (lithostatic pressure)	150 MPa	**6.1 km**
x_0 (H_2O)	5.0%	
P_i and depth (lithostatic pressure)	80 MPa	**3.3 km**
x_i (H_2O)	3.7%	
Magma intrusion: radius and total mass	**25 m**	175 10^6 kg
Initial crystallinity and total mass of melt[a]	55%	7.1 10^6 kg
Total mass of initial dissolved gas	~3.6 10^6 kg	
Mass of exsolved H_2O between P_0 and P_i	~1.0 10^6 kg[b]	
2) Crystallisation–degassing — 2nd degassing regime		
Melt vesicularity at Pi (α_i)[a]	4%	
Total mass of dissolved gas before crystallization	~2.6 10^6 kg	
Overpressure (tensile strength) limit	**0.2 MPa**	
Total number of degassing cycles	~30	

Bold values: input data; others: output values. Other parameters used in calculations are given in Annex 3 and 4.
[a] Parameters estimated from [42].
[b] To be compared to the estimated total mass of H_2O (~10^8 kg) produced during the 1976–1977 volcanic crisis.

strongly increases with crystallinity, and (ii), the temperature contrast between the magma and the surrounding rocks which decreases with time. Both effects contribute to an increase of the cycle duration with time. Detailed equations and fixed parameter values are given in Annex 4 and Table 3. Adjustable variables are intrusion dates and depth, total mass of magma and overpressure threshold. From discussions above, a depth of 3 km and a series of magma intrusions of rapidly increasing masses, from 1973 to July 1976 have been assumed (Table 3). The main part of the intrusion (85%) is emplaced during the culmination of the volcanic crisis in 1975–1976. The total mass of magma and the overpressure threshold have been adjusted in order to reproduce the time-series of Cl injections for the best resolved period (1976–1992): i.e. (i) the total duration, (ii) the time intervals between two successive injections and (iii) their relative mass fractions (Fig. 5b).

An intrusion of andesitic magma (H_2O-rich rhyolitic melt with ~55% crystals, T=900 °C, size~10^5 m^3) was emplaced at ~3 km depth between 1973 and July 1976 (mainly in 1975–1976). Degassing of this intrusion will occur in two phases: 1) by instantaneous decompression contemporaneous with magma injection from depth; and 2) by the cooling and crystallization of the intrusion after its stalling at shallow depth. A low overpressure threshold (0.2 MPa) is assumed to yield the large number of observed cycles before complete crystallization. This overpressure threshold is arbitrarily kept constant in the absence of sufficient information on the different processes that may modify it: e.g. weakening of surrounding rocks by successive rock-fracturing phases or consolidation and sealing by precipitation of hydrothermal minerals. The first degassing regime is dominant during the first period (1973–1976) and most part of the gas exsolved during the culmination of the volcanic crisis (1975–1976) have been lost directly to the atmosphere through the open vent. The intensified seismicity of mid-1973 and 1975–1976 may represent periods of high magma ascent rates and gas production. During the crystallization–degassing regime (1976–1992 period), the first degassing steps are rapid due to the high melt fraction and the large temperature contrast and cannot be completely resolved on the Cl time-series. They inject ~30% of the total mass of gas during the first 2 yr. Thereafter, it takes ~15 yr for complete magma crystallization and expulsion of the remaining gas fraction to occur.

The ranges of assumed mass of magma and calculated mass of H_2O vapour and Cl are consistent with the few quantitative estimates available for the 1975–

1976 volcanic crisis. The small volume (~10^5 m^3) of the inferred magma intrusion is consistent with the absence of a large thermal anomaly and of significant volcanic edifice deformation. It represents for example 0.1% of La Soufrière lava dome [20]. The calculated mass of magmatic H_2O expelled during magma intrusion represents ~2% of the total H_2O vapour production which has been roughly estimated for the 1975–1976 crisis at La Soufrière (P. Allard, personal communication) and which includes large fractions of hydrothermal and surficial waters vaporised during phreatic events. Finally, very similar ranges are found for the total amount of Cl transported in springs (~270 10^3 kg, Table 2) and the total amount of Cl in the initial melt (~180 10^3 kg) calculated from the model, assuming a mean [Cl] of ~2500 ppm [28].

8. Conclusion and perspectives

The chemical compositions of thermal springs around an active volcanic center represent a memory of the past volcanic activity. Halogen anomalies in the thermal springs characterise shallow degassing of volatile-rich andesitic magmas. The further the spring is located from the magma source, the older the recorded degassing events. This study shows that the 1976–1977 sismo-volcanic crisis at La Soufrière likely started ~3 yr before the onset of surface violent manifestations in 1976 by the intrusion of fresh magma at shallow depth. An evolution towards a major magmatic event could not have been discarded at that time. Long-term degassing in a pulsatory regime of this intrusion lasted ~15 yr. Geochemical survey of the water springs around the volcano some years before 1976, could have provided alerting information of the onset of a new magmatic activity. Renewed degassing from summit fumaroles began in 1992 associated with increased seismicity. This activity has shown a slow yet systematic increase starting in 1997 and has been associated thereafter with a sustained flux of HCl-rich vapour. It may thus represent the renewal of deep magmatic activity and thus deserves to be monitored and studied with great care. As shown for the 1976 crisis discussed in this paper, the permanent geochemical monitoring of La Soufrière volcano might provide in advance chemical signals associated with processes occurring deeper in the magmatic system.

Studies of recent volcanic crises in the Lesser Antilles arc show oscillatory and pulse like behaviours on short time scales (hours to months) for shallow magma degassing and lava dome extrusion (La Soufrière–this study–; Soufriere Hills [39]). Such cyclic behaviours are explained by fluid-dynamic models of degassing–crystallizing magmas in static [36] or flowing [33] regimes. The detailed and continuous records of eruptive activity over long periods of time (years) provide the best constraints on such models. For such purpose and for understanding future volcanic crises, geochemical monitoring, because it is simple and highly informative, is a highly valuable complement to geophysical observations.

Acknowledgments

We are grateful to S. Bigot, F. Beauducel, C. Auterives for their help in data acquisition and compilation and to the staff of the "Observatoire Volcanologique et Sismologique de la Guadeloupe" for their constant dedication to the hard suveillance tasks. We are indebted to M. Todesco and P. Allard for their constructive reviews. We also thank INSU-CNRS, France, for financial help in the acquisition and maintenance of the observatory analytical.

Appendix A. Annex 1: Geochemical monitoring

The temperature, pH, and major ion (pH, Na^+, K^+, Mg^{++}, Ca^{++}, F^-, Cl^-, SO_4^{--}, HCO_3^-) compositions have been measured in waters collected at a mean rate of 2–4 samples per month in 10 thermal springs [21,22,25,40]. Cl contents (and less systematically F contents) are measured just after sampling by ion chromatography. Br contents are measured by ICP-MS [16] in fresh samples since 1999 and in some selected archive samples. Exhaustive data are included in the Observatoires Volcanologiques Reports [21].

Appendix B. Annex 2: Advection–dispersion model

Considering an instantaneous injection of an amount dM_{Cl} of chlorine in a flowing aquifer, the

evolution of the concentration of injected Cl (C_{Cl}) with time and distance measured in the flow direction is given by:

$$C_{Cl}(x,\delta t) = (dM_{Cl})\left[4\Pi\delta t\sqrt{((Dx/\omega R)(Dy/\omega R))}\right]^{-1} \times \exp\left[-(x-\delta t U/\omega R)^2/(4\,\delta t\,Dx/\omega R)\right], \quad (1)$$

where x is the distance between the spring and the injection point taken along the flow direction, δt the interval of time between injection and measurement at point x, Dx and Dy are the coefficients of hydrodynamic dispersion in the directions perpendicular to x and y, U is the water flow velocity, ω the kinematic porosity, and R the retardation factor. It is generally assumed that dispersion coefficients are proportional to the groundwater velocity: $Dx=\alpha U$ and $Dy=\beta U$, with $\beta=\alpha/10$. The model assumes that transverse term (y) is negligible except for the dispersion coefficients. The used normalised flow rate value ($U/\omega R=10^{-5}$ ms^{-1}) is in the range of measurements in deep aquifers ([2–0.2] 10^{-5} ms^{-1}) and lower than that estimated by experiments of tracer injections in superficial aquifers of La Soufrière ($U/\omega R$ ~1.5 10^{-4} ms^{-1} [40]). This is consistent with the fact that the fluid transfer mostly occurs through the volcanic edifice which has a lower porosity than superficial deposits where circulate surficial aquifers.

Appendix C. Annex 3: Permeability controlled gas transfer

The characteristic time of gas transfer in a porous medium is given by:

$$t = \left(\mu_g/\kappa\right)\alpha_i\left(R^2/6\right)\left(1/Ps\right)\ln[(Pi-Ps)/(P-Ps)*P/Pi] \quad (2)$$

where μ_g is the gas viscosity (= 10^{-5} Pa s), κ the permeability (= 10^{-14} to 10^{-11} m^2), Pi and Ps are the initial magma pressure and the lithostatic pressure (100 and 80 MPa corresponding to depths of ~4 and ~3 km respectively), P is the magma pressure ($Pi>P>Ps$), R is a characteristic dimension parameter (R~10–100 m). α_i is the vesicularity of the melt acquired between an initial saturation pressure (P_0) and Pi. α_i is calculated by $\alpha_i=1/(1+Pi/[(x_0-x_i)\,\rho_{melt}(RT/M)])$. x values are the weight fractions of dissolved gas in the melt at pressure P and are calculated from the solubility law of H_2O in rhyolitic melts: $x=s\,P^n$, with s~4.11 10^{-6} and n~0.5. R, T and M are respectively the constant of perfect gases, the temperature and the molar weight of H_2O. Times are calculated to achieve complete decompression down to Ps ± 1 MPa.

Appendix D. Annex 4: Crystallization controlled degassing

Three equations describe this model: the first one describes the evolution of the crystal weight fraction ($f_s=m_s/M$, where m_s is the mass of crystals and M the total mass of magma) as a function of pressure (from [36]):

$$f_s \approx 1-(Pi/P)^n+(P/Pi-1)f_{gi}/x \quad (3a)$$

where f_{gi} represents the initial weight fraction of gas in the system; the second one assumes that f_s is linearly dependent on temperature (T) in the freezing range (from [38]):

$$df_s/dt = -1/(T_l-T_s)dT/dt \quad (3b)$$

where T_l and T_s represent the temperature of the liquidus (950 °C) and the solidus (750 °C), respectively. The third equation relates the evolution of the magma temperature as a function of the latent heat of crystallization (L=3.3 10^5 J/kg), the specific heat of the magma (Cp=1.5 10^3 J/kg/K), the Rayleigh number and the dimensions of the magma chamber (R) (from [38]):

$$dT/dt = -(A/R)(\alpha_{Th}g/v)^{1/3}\kappa^{2/3}(T-Tc)^{4/3}/(1+L/[Cp(T_l-T_s)]) \quad (3c)$$

where α_{Th} is the thermal expansion (= 5 10^{-5} K^{-1}), g the acceleration of gravity, A is a constant (taken equal to 0.2), κ the thermal diffusivity (= 10^{-6} ms^{-2}) and Tc is the temperature at the contact between the magma body (initial T=900 °C) and the surrounding (T_R=400 °C); $Tc=(T+T_R)/2$. The kinematic viscosity v is a key parameter since it may vary over a very

large range as a function of temperature but also as a function of the magma crystallinity. According to [41], a sigmoïdal variation of v as a function of crystallinity has been adopted (v range 10^{-2}–10^{10} m^2/s over the whole crystallinity range). It is assumed for simplification that inside magma body thermal energy is efficiently dissipated through magma convection. The overpressure evolution is calculated numerically and compared to a fracture criterion determined from the tensile strengths of volcanic structures which are in the range [0.1–5] MPa.

References

[1] M. Feuillard, C.J. Allègre, G. Brandeis, R. Gaulon, J.-L.L. Mouël, J.-C. Mercier, J.-P. Pozzi, M.P. Semet, The 1975–1977 crisis of La Soufrière de Guadeloupe (F.W.I.): a still-born magmatic eruption, J. Volcanol. Geotherm. Res. 16 (1983) 317–334.

[2] J. Zlotnicki, G. Boudon, J.-L.L. Mouël, The volcanic activity of La Soufrière of Guadeloupe (Lesser Antilles): structural and tectonic implications, J. Volcanol. Geotherm. Res. 49 (1992) 91–104.

[3] S.R. Young, R.S.J. Sparks, R. Robertson, L. Lynch, A.D. Miller, J. Shepherd, W.A. Aspinall, Overview of the eruption of Soufriere Hills, Montserrat, 18 July 1995 to December 1997, Geophys. Res. Lett. 25 (18) (1998) 3389–3392.

[4] P. Jackson, J.B. Shepherd, R.E. Robertson, G. Skerrt, Ground deformation studies at the Soufriere Hills volcano, Montserrat: I. electronic distance meter studies, Geophys. Res. Lett. 25 (18) (1998) 3409–3412.

[5] G. Chiodini, R. Cioni, A. Frullani, M. Guidi, L. Marini, F. Prati, B. Raco, Fluid geochemistry of Montserrat island, West Indies, Bull. Volcanol. 58 (1996) 380–392.

[6] G. Hammouya, P. Allard, P. Jean-Baptiste, F. Parello, M.P. Semet, S.R. Young, Pre- and syn-eruptive geochemistry of volcanic gases from Soufriere Hills of Montserrat, West Indies, Geophys. Res. Lett. 25 (19) (1998) 3685–3688.

[7] K.V. Cashman, R.P. Hoblitt, Magmatic precursors to the 18 May 1980 eruption of Mount St. Helens, USA, Geology 32 (2) (2004) 141–144.

[8] R.B. Symonds, W.I. Rose, G.J.S. Bluth, T.M. Gerlach, Volcanic-gas studies: methods, results and applications, in: M.R. Caroll, J.R. Holloway (Eds.), Volatiles in Magmas, Rev. Mineral., vol. 30, 1994, pp. 1–66 (Mineral. Soc. Amer.).

[9] R.B. Symonds, M.H. Reed, Calculation of multicomponent chemical equilibria in gas–solid–liquid systems: calculation methods, thermochemical data and applications to studies of high temperature volcanic gases with examples from Mount St. Helens, Am. J. Sci. 293 (1993) 758–864.

[10] W.F. Giggenbach, Geothermal solute equilibria. Derivation of Na–K–Mg–Ca geoindicators, Geochim. Cosmochim. Acta 52 (1988) 2749–2765.

[11] R.B. Symonds, T.M. Gerlach, M.H. Reed, Magmatic gas scrubbing: implications for volcano monitoring, J. Volcanol. Geotherm. Res. 108 (2001) 2749–2765.

[12] T.M. Gerlach, T.J. Casadevall, Fumarole emissions at Mount St. Helens volcano, June 1980 to October 1981: degassing of a magma-hydrothermal system, J. Volcanol. Geotherm. Res. 28 (1986) 141–160.

[13] W.F. Giggenbach, D. Tedesco, Y. Sulistiyo, A. Caprai, R. Cioni, R. Favara, T.P. Fisher, J.I. Hirabayashi, M. Korzhinsky, M. Martini, I. Menyailov, H. Shinohara, Evaluation of the results from the fourth and fifth IAVCEI field workshops on volcanic gases, Vulcano Island, Italy, and Java, Indonesia, J. Volcanol. Geotherm. Res. 108 (2001) 157–172.

[14] J.D. Webster, Water solubility and chlorine partitioning in Cl-rich granitic systems: effects of melt composition at 2 kbars and 800 °C, Geochim. Cosmochim. Acta 53 (1992) 2617–2630.

[15] B. Villemant, G. Boudon, H2O and halogen (F, Cl, Br) behaviour during shallow magma degassing processes, Earth Planet. Sci. Lett. 168 (1999) 271–286.

[16] A. Michel, B. Villemant, Determination of halogens (F, Cl, Br,I), sulphur and water in 17 reference geological material, Geostand. Newsl. 27 (2) (2003) 163–171.

[17] C. Oppenheimer, P. Francis, M. Burton, A.J.H. Maciejewski, L. Boardman, Remote measurement of volcanic gases by Fourier transform infrared spectroscopy, Appl. Phys. B67 (1998) 505–515.

[18] N. Bobrowski, G. Hönninger, B. Galle, U. Platt, Detection of bromine monoxide in volcanic plumes, Nature 423 (2003) 273–276.

[19] G. Boudon, M.P. Semet, P.M. Vincent, The evolution of la Grande Découverte (La Soufrière) volcano, Guadeloupe, F.W.I., in: J. Latter (Ed.), Volcano Hazards: Assessment and Monitoring, Springer-Verlag, 1989, pp. 86–109.

[20] J.C. Komorowski, G. Boudon, M. Semet, F. Beauducel, C. Anténor-Habazac, S. Bazin, G. Hammouya, Guadeloupe, in: J. Lindsay, R. Robertson, J. Shepherd, S. Ali (Eds.), Volcanic Hazard Atlas of the Lesser Antilles, University of the West Indies, Seismic Research Unit, Trinidad and IAVCEI, 2005, pp. 65–102.

[21] Observatoire_Volcanologique_et_Sismologique_de_la_Guadeloupe, Bilan Mensuel de l'Activité Volcanique et de la Sismicité régionale de l'Observatoire Volcanologique de la Soufriére (JCK 1999–2001, FB 2001–2005), IPGP, 1999–2005.

[22] S. Bigot, G. Hammouya, Surveillance hydrogéochimique de la Soufrière de Guadeloupe, 1978–1985: diminution de l'activité ou confinement? C. R. Acad. Sci., Paris 304 (Sér. II) (1987) 757–760.

[23] P. Allard, G. Hammouya, F. Parello, Dégazage magmatique diffus à la Soufrière de Guadeloupe, Antilles, C. R. Acad. Sci. Paris, Earth Planet. Sci. 327 (1998) 315–318.

[24] T. Brombach, L. Marini, J.-C. Hunziker, Geochemistry of the thermal springs and fumaroles of Basse-Terre Island, Guadeloupe, Lesser Antilles, Bull. Volcanol. 61 (2000) 477–490.

[25] IPGP, Rapports d'activité des Observatoires Volcanologiques des Antilles (Gadeloupe-Martinique). Nov. 1976–April 1977, April 1977–Dec. 1978, 1979, 1980, 1981, 1982, 1983–1984, IPGP, Paris, France.
[26] R.B. Symonds, W.I. Rose, T.M. Gerlach, P.H. Briggs, R.S. Harmon, Evaluation of gases, condensates, and SO2 emissions from Augustine volcano, Alaska: the degassing of a Cl-rich volcanic system, Bull. Volcanol. 52 (1990) 355–374.
[27] M. Edmonds, D. Pyle, C. Oppenheimer, HCl emission at Soufriere Hills volcano, Montserrat, West Indies, during a second phase of dome building: November 1999 to October 2000, Bull. Volcanol. 64 (2002) 21–30.
[28] B. Villemant, G. Boudon, S. Nougrigat, S. Poteaux, A. Michel, H2O and halogen in volcanic clasts: tracers of degassing processes during plinian and dome-forming eruptions, in: C. Oppenheimer, D. Pyle, J. Barclay (Eds.), Volcanic Degassing, Geol. Soc. London, vol. 213, Special Publication, 2003, pp. 63–79.
[29] A. Hirn, B. Michel, Evidence of migration of main shocks during seismovolcanic crisis of La Soufrière (Guadeloupe, Lesser Antilles) in 1976, J. Volcanol. Geotherm. Res. 6 (1979) 295–304.
[30] M. Todesco, G. Chiodini, G. Macedonio, Monitoring and modelling hyfrothermal fluid emission at La Solfatara (Phlegrean Fields, Italy); an interdisciplinary approach to the study of diffuse degassing, J. Volcanol. Geotherm. Res. 125 (2003) 57–79.
[31] C. Jaupart, C.J. Allègre, Gas content, eruption rate and instabilities in silicic volcanoes, Earth Planet. Sci. Lett. 102 (1991) 413–429.
[32] R.S.J. Sparks, Causes and consequences of pressurisation in lava dome eruptions, Earth Planet. Sci. Lett. 150 (1997) 37–41.
[33] M. Melnik, R.S.J. Sparks, Nonlinear dynamics of lava dome extrusion, Nature 402 (1999) 37–41.
[34] J.E. Hammer, K.V. Cashman, R.P. Hoblitt, S. Newman, Degassing and microlite crystallization during the pre-climactic events of the 1991 eruption of the Pt. Pinatubo, Philippines, Bull. Volcanol. 60 (1999) 355–380.
[35] S. Blake, Volatile oversaturation during the evolution of silicic magma chambers as an eruption trigger, J. Geophys. Res. 89 (1984) 8237–8244.
[36] S. Tait, C. Jaupart, S. Vergniolle, Pressure, gas content and eruption periodicity of a shallow, crystallising magma chamber, Earth Planet. Sci. Lett. 92 (1989) 107–123.
[37] F. Spera, Thermal evolution of plutons: a parametrized approach, Science 207 (1980) 299–301.
[38] G. Brandeis, C. Jaupart, On the interaction between convection and crystallization in cooling magma chambers, Earth Planet. Sci. Lett. (1986) 345–361.
[39] B. Voight, et al., Magma flow instability and cyclic activity at Soufriere Hills volcano, Monserrat, West Indies, Science 283 (1999) 1138–1142.
[40] S. Bigot, G. Boudon, M.P. Semet, G. Hammouya, Traçage chimique de la circulation des eaux souterraines sur le volcan de la Grande Découverte (la Soufrière), Guadeloupe, C. R. Acad. Sci., Paris 318 (Sér. II) (1994) 1215–1221.
[41] A.-M. Lejeune, P. Richet, Rheology of crystal bearing silicate melts: an experimental study at high viscosities, J. Geophys. Res. 100 (1995) 4215–4229.
[42] B. Villemant, G. Boudon, Transition between dome-forming and plinian eruptive styles: H2O and Cl degassing behaviour, Nature 392 (1998) 65–69.